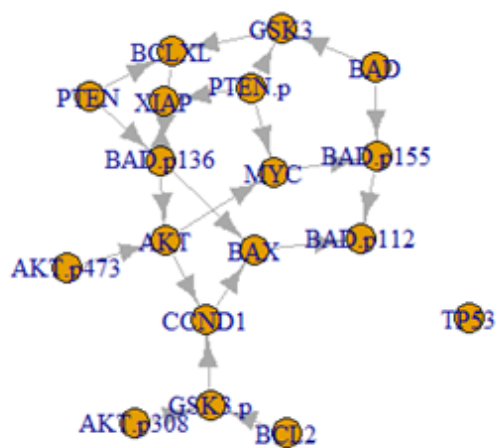


Graphical Abstract

Adaptive Bayesian Structure Learning of DAGs With Non-conjugate Prior

S. Nazari¹, M. Arashi², A. Sadeghkhanian³



¹Email: asemaneh1369@gmail.com

²Corresponding Author, Email: arashi@um.ac.ir

³Email: asadeghkhanian@ncat.edu

Highlights

Adaptive Bayesian Structure Learning of DAGs With Non-conjugate Prior

S. Nazari⁴, M. Arashi⁵, A. Sadeghkhanian⁶

- We develop a Bayesian structure learning of DAGs with high posterior probability.
- We combat computational burden of the Gaussian DAG learning with non-conjugate priors.
- The proposed Bayesian structure learning of Gaussian DAGs include nodes if the inclusion probability is high, unlike the case of using conjugate priors.

⁴Email: asemaneh1369@gmail.com

⁵Corresponding Author, Email: arashi@um.ac.ir

⁶Email: asadeghkhanian@ncat.edu

Adaptive Bayesian Structure Learning of DAGs With Non-conjugate Prior

S. Nazari^{1a}, M. Arashi^{2a}, A. Sadeghkhanian^{3b}

^aDepartment of Statistics, Faculty of Mathematical Sciences, Ferdowsi University of Mashhad, Iran,

^bDepartment of Mathematics and Statistics, North Carolina Agricultural and Technical State University, USA,

Abstract

Abstract: Directed Acyclic Graphs (DAGs) are solid structures used to describe and infer the dependencies among variables in multivariate scenarios. Having a thorough comprehension of the accurate DAG-generating model is crucial for causal discovery and estimation. Our work suggests utilizing a non-conjugate prior for Gaussian DAG structure learning to enhance the posterior probability. We employ the idea of using the Bessel function to address the computational burden, providing faster MCMC computation compared to the use of conjugate priors. In addition, our proposal exhibits a greater rate of adaptation when compared to the conjugate prior, specifically for the inclusion of nodes in the DAG-generating model. Simulation studies demonstrate the superior accuracy of DAG learning, and we obtain the same maximum a posteriori and median probability model estimate for the AML data, using the non-conjugate prior.

Keywords: Bayesian structure learning, Directed acyclic graph, Graphical model, Normal-gamma prior, Posterior probability.

1. Introduction

Probabilistic graphical models have evolved as powerful and useful tools for modeling and inferring dependent relations in complicated multivari-

¹Email: asemaneh1369@gmail.com

²Corresponding Author, Email: arashi@um.ac.ir

³Email: asadeghkhanian@ncat.edu

ate environments over the last few decades ([19]). Directed acyclic graphs (DAGs), also known as Bayesian networks, are widely employed to infer a specific set of conditional independence relationships between variables, holding the DAG Markov property. A DAG imposes a set of conditional independencies between variables through a DAG-dependent factorization of the joint distribution and provides an effective tool to read-off such relations directly from the graph using some criteria. Real data problems generally show that the set of conditional dependencies among variables cannot be assumed in advance, which makes the DAG-generating model unknown. In numerous fields, DAG structural learning is the fundamental objective of the analysis since it helps uncover dependence relationships that can aid in understanding the behavior of variables; see for instance [13] and [29]. Furthermore, when DAGs combined with the do-calculus theory ([24]), DAGs can potentially be used for causal inference, which facilitates the identification and estimation of relationships of causality between variables. When DAGs are provided with causal assumptions, the process of learning their graphical structure is commonly referred to as causal structure learning or simply causal discovery ([20] and [27]). Given faithfulness and causal sufficiency ([31]), the DAG structure can only be learned up to its Markov equivalence class ([1]), which assembles all DAGs with the same Markov property. However, because equivalent DAGs still reflect different structural causal models (SCMs), see [24], the identified Markov equivalence class can be used for recovering a collection of potentially distinct causal effects. This issue may be addressed from a statistical standpoint by using a model selection approach, and numerous approaches have been presented in this regard.

From a Bayesian perspective, DAG structure learning has generally been treated as a Bayesian model selection. In this framework, Bayesian methodologies for DAG structural learning involve estimating a posterior distribution over the space of graphs. This approach provides a coherent quantification of the uncertainty around the data-generating model. Markov Chain Monte Carlo (MCMC) techniques are often employed to estimate the posterior distribution of graph structures, as exemplifies in studies such as [11], [23], [4], [9] and [5]. Conversely, Bayesian methods require prior elicitation for each model dependent parameter which is subject to constraints imposed by the conditional independencies of the underlying DAG structure, as discusses in [14]. From this perspective, prior distribution specification plays important role. In [9], a normal-inverse-gamma conjugate prior is employed for structure learning of Gaussian DAGs. Generally, conjugate priors offer tractable ana-

lytical computation, easing MCMC computations. In this study, we employ non-conjugate normal-gamma prior, following [2], to achieve higher posterior probability and improve some graphical metrics in structure learning of Gaussian DAGs. We demonstrate that our approach exhibits a conservative behavior in term of edge inclusion in the Gaussian DAG (refer to Table 3 and the subsequent discussion) and provides faster computation compared to the normal-inverse-gamma model. Additionally [21], [22] and [34] investigate Bayesian structure learning in undirected Gaussian graphical models.

The organization of the rest of this study is as follows. In section 2, we give some preliminary results on graphical models and DAGs building on the Bayesian structure studied in [9]. Section 3 gives posterior probabilities and marginal distributions for the normal-gamma prior on the Gaussian DAG parameters. An MCMC algorithm is given in section 4, while Section 5 contains numerical analyses. We conclude our study in section 6, with the proof of main result is provided in Appendix.

2. Preliminaries

In this section, we present fundamental concepts of DAGs and graph theory. Readers are referred to [19] and [25] for details.

2.1. Gaussian DAG-models

Consider $\mathcal{D} = (V, E)$ be a Directed Acyclic Graph (DAG), with $V = \{1, \dots, q\}$ representing a collection of vertices (or nodes) and $E \subseteq V \times V$ is a set of edges. If $(u, v) \in E$, \mathcal{D} contains the directed edge $u \rightarrow v$. Furthermore, \mathcal{D} cannot have cycles, that is paths of form $u_0 \rightarrow u_1 \rightarrow \dots \rightarrow u_k$ where $u_0 \equiv u_k$. For a given DAG \mathcal{D} , if there is an edge $u \rightarrow v$ we say that u is a *parent* of v (conversely, v is a child of u) and denote the parent set of v in \mathcal{D} as $pa_{\mathcal{D}}(v)$, while the set $fa_{\mathcal{D}}(v) = v \cup pa_{\mathcal{D}}(v)$ is called the *family* of v in \mathcal{D} . Furthermore, a DAG is *complete* if all its nodes are joined by edges. Finally, a DAG \mathcal{D} can be uniquely expressed by its (q, q) *adjacency matrix* $\mathbf{A}^{\mathcal{D}}$ such that $\mathbf{A}_{u,v}^{\mathcal{D}} = 1$ if and only \mathcal{D} contains $u \rightarrow v$ and 0 otherwise. A DAG \mathcal{D} encodes a set of conditional independencies between nodes(variables) that can be read-off from the DAG using graphical criteria, such as *d-separation* [24]. The DAG Markov property is defined by the resulting set of conditional independence encoded in \mathcal{D} .

In the following, we define a Gaussian DAG-model in terms of likelihood and prior distributions for model parameters.

Let $\mathcal{D} = (V, E)$ be a DAG, $\mathbf{x} = (x_1, \dots, x_q)^T$ a collection of real-valued random variables each associated to a node in V . Also assume that the joint density of $(x_1, \dots, x_q)^T$ belongs to a zero-mean Gaussian DAG-model, namely

$$\mathbf{x} \mid \Omega_{\mathcal{D}} \sim \mathcal{N}_q(\mathbf{0}, \Omega_{\mathcal{D}}^{-1}), \quad \Omega_{\mathcal{D}} \in \mathcal{P}_{\mathcal{D}}, \quad (1)$$

where $\Omega_{\mathcal{D}} = \Sigma_{\mathcal{D}}^{-1}$ is the precision (inverse-covariance) matrix, and $\mathcal{P}_{\mathcal{D}}$ is the space of symmetric positive definite (s.p.d) precision matrices Markov w.r.t. \mathcal{D} . Therefore, $\Omega_{\mathcal{D}}$ satisfies the conditional independencies (Markov property) embedded by \mathcal{D} .

According to modified Cholesky decomposition of $\Omega = \Sigma^{-1}$, that is $\Omega = \mathbf{L}\mathbf{D}^{-1}\mathbf{L}^T$, model (1) can be written as follows:

$$\mathbf{L}^T(x_1, \dots, x_q)^T = \boldsymbol{\varepsilon}, \quad \boldsymbol{\varepsilon} \sim \mathcal{N}_q(\mathbf{0}, \mathbf{D}), \quad (2)$$

where \mathbf{L} is a $q \times q$ matrix of coefficients that has a value for every (u, v) -element \mathbf{L}_{uv} with $u \neq v$, $\mathbf{L}_{uv} \neq 0$ if and only if $(u, v) \in E$, whereas $\mathbf{L}_{uu} = 1$ for each $u = 1, \dots, q$. Also \mathbf{D} is a $q \times q$ diagonal matrix with (u, u) -element \mathbf{D}_{uu} .

As a result, it deduces a re-parameterization of $\Omega = \Sigma^{-1}$ in relation to the node-parameters $\{(\mathbf{D}_{jj}, \mathbf{L}_{\prec j}), j = 1, \dots, q\}$, such that

$$\mathbf{L}_{\prec j} = -\Sigma_{\prec j \succ}^{-1} \Sigma_{\prec j}, \quad \mathbf{D}_{jj} = \Sigma_{jj|pa_{\mathcal{D}}(j)},$$

Where $\Sigma_{jj|pa_{\mathcal{D}}(j)} = \Sigma_{jj} - \Sigma_{[j \succ} \Sigma_{\prec j \succ}^{-1} \Sigma_{\prec j]}$, $\prec j] = pa_{\mathcal{D}}(j) \times j$, $[j \succ = j \times pa_{\mathcal{D}}(j)$, $\prec j \succ = pa_{\mathcal{D}}(j) \times pa_{\mathcal{D}}(j)$. As well parameter \mathbf{D}_{jj} represents the conditional variance of x_j , $\text{Var}(x_j \mid \mathbf{x}_{pa_{\mathcal{D}}(j)})$. For further details refer to [9]. Model (1) can be re-written as follows based on (2):

$$f(x_1, \dots, x_q \mid \mathbf{D}, \mathbf{L}) = \prod_{j=1}^q d\mathcal{N}(x_j \mid -\mathbf{L}_{\prec j}^T \mathbf{x}_{pa_{\mathcal{D}}(j)}, \mathbf{D}_{jj}). \quad (3)$$

Now consider n random samples $\mathbf{x}_i = (x_{i,1}, \dots, x_{i,q})^T \in \mathbb{R}^q$, $i = 1, \dots, n$, from (3), and suppose $\mathbf{X} = (\mathbf{x}_1, \dots, \mathbf{x}_n)^T$ be the $n \times q$ data matrix. The likelihood function is given by

$$\begin{aligned} f(\mathbf{X} \mid \mathbf{D}, \mathbf{L}) &= \prod_{i=1}^n f(x_{i,1}, \dots, x_{i,q} \mid \mathbf{D}, \mathbf{L}) \\ &= \prod_{j=1}^q d\mathcal{N}_n(\mathbf{X}_j \mid -\mathbf{X}_{pa_{\mathcal{D}}(j)} \mathbf{L}_{\prec j}, \mathbf{D}_{jj} \mathbf{I}_n), \end{aligned} \quad (4)$$

where \mathbf{X}_A is the $n \times |A|$ sub-matrix of \mathbf{X} corresponding to the set A of columns of \mathbf{X} and \mathbf{I}_n denotes the $n \times n$ identity matrix.

In a recent study, [9] introduced a conjugate prior for node-parameters $\{(\mathbf{D}_{jj}, \mathbf{L}_{\prec j})\}$, $j = 1, \dots, q$, that are priori independent with distribution

$$\begin{aligned} \mathbf{D}_{jj} \mid \mathcal{D} &\sim \Gamma^{-1} \left(\frac{1}{2} \alpha_j^{\mathcal{D}}, \frac{1}{2} \mathbf{U}_{jj|pa_{\mathcal{D}}(j)} \right), \\ \mathbf{L}_{\prec j} \mid \mathbf{D}_{jj}, \mathcal{D} &\sim \mathcal{N}_{|pa_{\mathcal{D}}(j)|} \left(-\mathbf{U}_{\prec j}^{-1} \mathbf{U}_{\prec j}, \mathbf{D}_{jj} \mathbf{U}_{\prec j}^{-1} \right), \end{aligned} \quad (5)$$

where \mathbf{U} is the rate hyperparameter (a $q \times q$ symmetric positive definite matrix) and $\boldsymbol{\alpha}^{\mathcal{D}} = (\alpha_1^{\mathcal{D}}, \dots, \alpha_q^{\mathcal{D}})^T$ is the shape hyperparameter according to [3]. The default selection, $\alpha_j^{\mathcal{D}} = \alpha + |pa_{\mathcal{D}}(j)| - q + 1$, ($\alpha > q - 1$) ensures compatibility amongst prior distributions for Markov equivalent DAGs. It can be demonstrated, in specific, that with this choice, any two Markov equivalent DAGs are allocated the same marginal likelihood.

3. Normal-Gamma Prior

In this section, we change the distribution of diagonal elements $\mathbf{D}_{jj} = \boldsymbol{\Sigma}_{jj|pa_{\mathcal{D}}(j)}$ and compute the marginal and posterior density functions. Specifically, we replace the inverse gamma with the gamma distribution.

Assume

$$\begin{aligned} \mathbf{D}_{jj} \mid \mathcal{D} &\sim \Gamma \left(\frac{1}{2} \alpha_j^{\mathcal{D}}, \frac{1}{2} \mathbf{U}_{jj|pa_{\mathcal{D}}(j)} \right), \\ \mathbf{L}_{\prec j} \mid \mathbf{D}_{jj}, \mathcal{D} &\sim \mathcal{N}_{|pa_{\mathcal{D}}(j)|} \left(-\mathbf{U}_{\prec j}^{-1} \mathbf{U}_{\prec j}, \mathbf{D}_{jj} \mathbf{U}_{\prec j}^{-1} \right), \end{aligned} \quad (6)$$

is a prior on parameters $\{(\mathbf{D}_{jj}, \mathbf{L}_{\prec j})\}$, $j = 1, \dots, q$.

Further, assume the prior on (\mathbf{D}, \mathbf{L}) is given by

$$p(\mathbf{D}, \mathbf{L} \mid \mathcal{D}) = \prod_{j=1}^q p(\mathbf{L}_{\prec j} \mid \mathbf{D}_{jj}) p(\mathbf{D}_{jj}). \quad (7)$$

In the following, we present the posterior distribution of node-parameters and marginal likelihood of each node in DAG \mathcal{D} .

Theorem 1. Assuming equations (4) and (7), the node-marginal likelihood is given by

$$m(\mathbf{X}_j | \mathbf{X}_{pa_{\mathcal{D}}(j)}, \mathcal{D}) = (2\pi)^{-\frac{n}{2}} \times \frac{|\mathbf{U}_{\prec j \succ}|^{\frac{1}{2}}}{|\tilde{\mathbf{U}}_{\prec j \succ}|^{\frac{1}{2}}} \times \frac{\left(\frac{1}{2}\mathbf{U}_{jj|pa_{\mathcal{D}}(j)}\right)^{\frac{1}{2}\alpha_j^{\mathcal{D}}}}{\Gamma\left(\frac{1}{2}\alpha_j^{\mathcal{D}}\right)} \\ \times 2K_a\left(2\sqrt{\alpha\beta}\right) \left(\frac{\alpha}{\beta}\right)^{\frac{a}{2}}.$$

See the Appendix for the proof.

Theorem 2. Under the assumptions of section 2, assume (7) for the prior on (\mathbf{D}, \mathbf{L}) . Then the joint posterior density function of (\mathbf{D}, \mathbf{L}) given the data \mathbf{X} , $p(\mathbf{D}, \mathbf{L} | \mathcal{D}, \mathbf{X})$, for $j = 1, \dots, q$ is

$$p(\mathbf{L}_{\prec j} | \mathbf{D}_{jj}, \mathcal{D}, \mathbf{X}) = (2\pi)^{-\frac{|pa_{\mathcal{D}}(j)|}{2}} \mathbf{D}_{jj}^{-\frac{|pa_{\mathcal{D}}(j)|}{2}} |\tilde{\mathbf{U}}_{\prec j \succ}|^{\frac{1}{2}} \exp\left\{-\frac{1}{2\mathbf{D}_{jj}} (\mathbf{L}_{\prec j} - \mathbf{M}^{-1}\mathbf{b})^T \mathbf{M} (\mathbf{L}_{\prec j} - \mathbf{M}^{-1}\mathbf{b})\right\},$$

$$p(\mathbf{D}_{jj} | \mathcal{D}, \mathbf{X}) = \frac{\mathbf{D}_{jj}^{\frac{1}{2}\alpha_j^{\mathcal{D}} - \frac{n}{2} - 1} \exp\left\{-\frac{1}{2}\mathbf{U}_{jj|pa_{\mathcal{D}}(j)}\mathbf{D}_{jj} - \frac{1}{2\mathbf{D}_{jj}} \left[-\mathbf{b}^T \mathbf{M}^{-1}\mathbf{b} + \mathbf{U}_{\prec j}^T \mathbf{U}_{\prec j}^{-1} \mathbf{U}_{\prec j} + \mathbf{X}_j^T \mathbf{I}_n \mathbf{X}_j\right]\right\}}{2K_a(2\sqrt{\alpha\beta}) \left(\frac{\alpha}{\beta}\right)^{\frac{a}{2}}},$$

where

$$\mathbf{M} = \tilde{\mathbf{U}}_{\prec j \succ} = \mathbf{U}_{\prec j \succ} + \mathbf{X}_{pa_{\mathcal{D}}(j)}^T \mathbf{I}_n \mathbf{X}_{pa_{\mathcal{D}}(j)}, \mathbf{b} = -\mathbf{X}_{pa_{\mathcal{D}}(j)}^T \mathbf{I}_n \mathbf{X}_j - \mathbf{U}_{\prec j}, a = \frac{1}{2}\alpha_j^{\mathcal{D}} - \frac{n}{2}, \\ \alpha = \frac{1}{2} \left[-\mathbf{b}^T \mathbf{M}^{-1}\mathbf{b} + \mathbf{U}_{\prec j}^T \mathbf{U}_{\prec j}^{-1} \mathbf{U}_{\prec j} + \mathbf{X}_j^T \mathbf{I}_n \mathbf{X}_j\right], \beta = \frac{1}{2}\mathbf{U}_{jj|pa_{\mathcal{D}}(j)},$$

and $K_\nu(\cdot)$ is the Bessel function of the third kind.

The proof directly follows from Theorem 1 and is omitted for the sake of saving space.

4. MCMC Scheme

In this section, we detail the MCMC scheme to generate samples from the posterior distribution

$$p(\mathbf{D}, \mathbf{L}, \mathcal{D} \mid \mathbf{X}) \propto f(\mathbf{X} \mid \mathbf{D}, \mathbf{L}, \mathcal{D}) p(\mathbf{D}, \mathbf{L} \mid \mathcal{D}) p(\mathcal{D}), \quad (8)$$

where, following [9] to each DAG $\mathcal{D} \in \mathcal{S}_q$, the set of all DAGs on q nodes, we assume $p(\mathcal{D}) \propto p(\mathbf{S}^{\mathcal{D}})$ with

$$p(\mathbf{S}^{\mathcal{D}}) = \pi^{|\mathbf{S}^{\mathcal{D}}|} (1 - \pi)^{\frac{q(q-1)}{2} - |\mathbf{S}^{\mathcal{D}}|}, \quad (9)$$

where $\mathbf{S}^{\mathcal{D}}$ is the (symmetric) 0 – 1 adjacency matrix of the skeleton of the DAG, $|\mathbf{S}^{\mathcal{D}}|$ is the number of edges in the skeleton, $\pi \in [0, 1]$ prior probability of edge inclusion and $q(q-1)/2$ corresponds to the maximum number of edges in a DAG on q nodes.

In the first step, at each iteration of the MCMC scheme, we start defining a new DAG \mathcal{D}' from a suitable proposal distribution $q(\mathcal{D}' \mid \mathcal{D})$ on the DAG space, determining the transitions between DAGs within the space \mathcal{S}_q .

To do this, we examine three types of operators that locally modify an input DAG \mathcal{D} . These operators include inserting a directed edge (InsertD $u \rightarrow v$ for short), deleting a directed edge (DeleteD $u \rightarrow v$), and reversing a directed edge (ReverseD $u \rightarrow v$). For each $\mathcal{D} \in \mathcal{S}_q$, we then construct the set of *valid* operators $\mathcal{O}_{\mathcal{D}}$, that is operators whose resulting graph is a DAG. Therefore, given the current \mathcal{D} we suggest \mathcal{D}' by uniformly sampling a DAG in $\mathcal{O}_{\mathcal{D}}$. Due to one-one correspondence between each operator and resulting DAG \mathcal{D}' , the probability of transition is given by $q(\mathcal{D}' \mid \mathcal{D}) = 1/|\mathcal{O}_{\mathcal{D}}|$.

Algorithm 1: Production of $\mathcal{O}_{\mathcal{D}}$ and sampling of \mathcal{D}' from $q(\mathcal{D}' | \mathcal{D})$

input : A DAG \mathcal{D}
output: The collection of valid operators $\mathcal{O}_{\mathcal{D}}$, a DAG \mathcal{D}' taken from $q(\mathcal{D}' | \mathcal{D})$

- 1 Construct:
- 2 $I_{\mathcal{D}}$, the set of all possible operators of type InsertD,
- 3 $E_{\mathcal{D}}$, the set of all possible operators of type DeleteD,
- 4 $R_{\mathcal{D}}$, the set of all possible operators of type ReverseD;
- 5 **for** each operator $o_D \in I_{\mathcal{D}}$ **do**
- 6 | add o_D to $\mathcal{O}_{\mathcal{D}}$ if o_D is valid
- 7 **end**
- 8 **for** each operator $o_D \in E_{\mathcal{D}}$ **do**
- 9 | add o_D to $\mathcal{O}_{\mathcal{D}}$ if o_D is valid
- 10 **end**
- 11 **for** each operator $o_D \in R_{\mathcal{D}}$ **do**
- 12 | add o_D to $\mathcal{O}_{\mathcal{D}}$ if o_D is valid
- 13 **end**
- 14 Draw uniformly an operator o_D from $\mathcal{O}_{\mathcal{D}}$ and obtain \mathcal{D}' by applying it to \mathcal{D}

On the other hand, to update the DAGs, due to the structure of proposal distribution, when proposing a DAG \mathcal{D}' which differs from the current graph \mathcal{D} by one edge (h, j) , we will need to compare two DAGs \mathcal{D} and \mathcal{D}' . Therefore, using Theorem 1, $q(\mathcal{D}' | \mathcal{D}) = 1/|\mathcal{O}_{\mathcal{D}}|$, and (9) the acceptance probability for \mathcal{D}' is given by

$$\alpha_{\mathcal{D}'} = \min \left\{ 1, \frac{m(\mathbf{X}_j | \mathbf{X}_{pa_{\mathcal{D}'}(j)}, \mathcal{D}')}{m(\mathbf{X}_j | \mathbf{X}_{pa_{\mathcal{D}}(j)}, \mathcal{D})} \cdot \frac{p(\mathcal{D}')}{p(\mathcal{D})} \cdot \frac{q(\mathcal{D} | \mathcal{D}')}{q(\mathcal{D}' | \mathcal{D})} \right\}. \quad (10)$$

Algorithm 2 summarizes our MCMC scheme for posterior inference on DAGs and DAG-parameters. In this context, let S , B , \mathbf{X} , α , \mathbf{U} and w denote respectively, the number of final MCMC draws from the posterior, the burn-in period, the $n \times q$ data matrix, the hyperparameters of the prior distribution and the prior probability of edge inclusion.

Algorithm 2: MCMC scheme to sample from the posterior of DAGs and parameter

input : $S, B, \mathbf{X}, \alpha, \mathbf{U}, w$
output: S samples from the posterior distribution (8)

- 1 Initialize \mathcal{D}^0 , e.g. the empty DAG;
- 2 **for** $s = 1, \dots, B + S$ **do**
- 3 Sample \mathcal{D}' from $q(\mathcal{D}' | \mathcal{D}^{(s-1)})$ using Algorithm 1;
- 4 Set $\mathcal{D}^{(s)} = \mathcal{D}'$ with probability (10), otherwise $\mathcal{D}^{(s)} = \mathcal{D}^{(s-1)}$;
- 5 Sample $(\mathbf{D}^{(s)}, \mathbf{L}^{(s)})$ from its full conditional

$$p(\mathbf{D}^{(s)}, \mathbf{L}^{(s)} | \mathcal{D}^{(s)}, \mathbf{X}) = \prod_{j=1}^q p(\mathbf{L}_{\prec j}^{(s)} | \mathbf{D}_{jj}^{(s)}, \mathcal{D}^{(s)}, \mathbf{X}) p(\mathbf{D}_{jj}^{(s)} | \mathcal{D}^{(s)}, \mathbf{X});$$
- 6 **end**
- 7 **return** $\{(\mathbf{D}^{(s)}, \mathbf{L}^{(s)}, \mathcal{D}^{(s)}), s = B + 1, \dots, B + S\}$

5. Numerical Analysis

In this section, we compare our methodology with [9], which we henceforth refer to as the Normal-Gamma (NG) model for easier reference, alongside the Normal-Inverse-Gamma (NIG) model.

5.1. Simulation study

The performance of our method is assessed through simulated data, with various scenarios considered by varying the sample size $n \in \{200, 300\}$ and the number of nodes $q \in \{40, 50\}$. We generate 40 DAGs using a probability of edge inclusion equal to $3/2q - 2$ to induce sparsity; see [26]. Then, for each DAG \mathcal{D} , we continue as follows. We fix $\mathbf{D}^{\mathcal{D}} = \mathbf{I}_q$ and then following [7], we randomly draw the non-zero elements of $\mathbf{L}^{\mathcal{D}}$ in the interval $[-2, -1] \cup [1, 2]$. We finally construct the precision matrix $\mathbf{\Omega} = \mathbf{L}\mathbf{D}^{-1}\mathbf{L}^T$ and generate n random samples from the Gaussian DAG-model $\mathcal{N}_q(0, \mathbf{\Omega}_{\mathcal{D}}^{-1})$.

The performance in learning the graphical structure of the DAG is evaluated by computing the misspecification rate (MISR), specificity (SP), sensitivity (SE), false negative rate (FNR), accuracy (AC) and the F1-score (F1) as defined in Table 1. The number of true positive (TP), true negative (TN), false positive (FP), and false negative (FN) are denoted accordingly. Better classification performance is implied by values of specificity, sensitivity, accuracy and F1-score closer to one. The closer the values of the false negative

rate and misspecification rate are to zero, the better.

Measure	Performance function
SP	$\frac{TN}{TN+FP}$
SE	$\frac{TP}{TP+FN}$
FNR	$\frac{FP}{FP+TN}$
F1	$\frac{TP}{TP+1/2(FP+FN)}$
MISR	$\frac{FP+FN}{q(q-1)}$
AC	$\frac{TP}{TP+FN}$

Table 1: Performance measures used to compare NIG and NG prior models in DAG structure learning.

	n=200		n=300	
	NIG	NG	NIG	NG
$q = 40$				
SP	0.9811	0.998	0.978	0.994
SE	0.608	0	0.577	0.001
FNR	0.0186	0.001	0.021	0.005
F1	0.476	0	0.441	0.002
MISR	0.0262	0.020	0.029	0.024
AC	0.9744	0.980	0.970	0.975
$q = 50$				
SP	0.9813	0.999	0.980	0.996
SE	0.527	0.0005	0.541	0.0007
FNR	0.0188	0.0006	0.019	0.003
F1	0.392	0.041	0.389	0.044
MISR	0.0264	0.016	0.026	0.018
AC	0.974	0.984	0.974	0.981

Table 2: Performance measure for the simulated data for NIG and NG with number of nodes $q \in \{40, 50\}$ and sample size $n \in \{200, 300\}$.

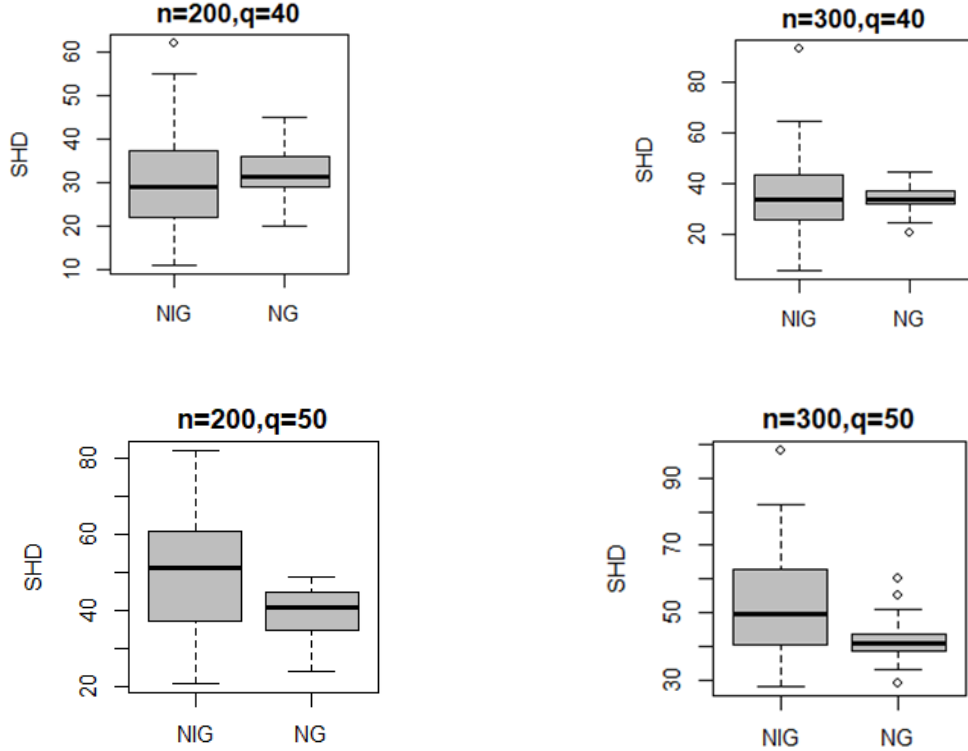


Figure 1: Boxplots of the SHD between the estimated DAG and the true DAG.

Table 2 reflects that the SP, FNR, MISR, and AC measures for our model have improved when compared to the model based on the NIG prior. According to Figure 1, the structural Hamming distances (SHD) indicate that our model is superior since the amount of variations in SHD values for our model are less compared to the NIG model. However, it's noteworthy that the SE and F1 values of the NG prior are lower when compared to the model NIG. This is attributed to the fact that our model has a very low TP, nearly approaching zero. Obtaining such results appears logical because we considered $3/2q - 2 = 0.03$, that is, we considered the prior probability of edge inclusion in the model to be low, so the number of 1 values in the model decreases, causing the TP values of our model to shrink.

To demonstrate the impact of increasing w on the results, similar to [8], we set $w = 0.2$. That is, we increase the probability of edge inclusion in the

DAG. As indicated in Table 3, the outcome is denser DAGs compared to the previous configuration.

	NIG	NG
SE	0.42	0.006
F1	0.303	0.012

Table 3: SE and F1 values for the NIG and NG prior with $q = 40$ and $n = 200$.

In conclusion, the proposed method is more conservative in the inclusion of edges compared with the NIG prior model, as indicated by its lower sensitivity and F1-score. To elaborate more, in what follows, we show that it is possible to achieve larger values than those of Table 3 for the SE and F1 in model. To this end, knowing that graph structures are not often used for DAGs, we computed these two measures for three well-known structures. Table 4 illustrates how one achieves larger SE and F1 values using the proposed prior structure.

Graph structure	SE	F1
Random	0.13	0.21
Hub	0.21	0.11
Band	0.16	0.22

Table 4: The SE and F1 values, for the NG prior with $q = 40$ and $n = 200$.

Finally, Figure 2 represents the computational time (CT) (averaged over 10 replicates) per iteration, as a function of $q \in \{5, 10, 20, 50, 100\}$ for $n = 500$ (left panel), and as a function of $n \in \{50, 100, 200, 300, 500\}$ for $q = 50$ (right panel). Surprisingly, the CT of our method increases with the number of variables and sample size, but it remains generally lower than that of the NIG model. Reflecting the Bessel function in the posterior and marginal models does not add computational delay or complexity.

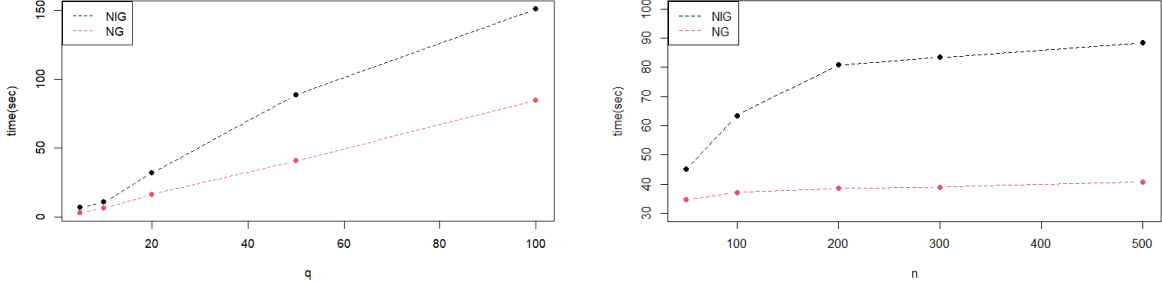


Figure 2: Computational time (in seconds) per iteration, as a function of the number of variables q for fixed $n = 500$ (left plot) and as a function of the sample size n for fixed $q = 50$ (right plot), averaged over 10 replicates.

5.2. Leukemia data analysis

In this subsection, we consider a biological dataset concerning patients affected by Acute Myeloid Leukemia (AML). AML represents an aggressive hematological cancer characterized by uncontrolled proliferation of hematopoietic stem cells in the bone marrow. AML responds very poorly to chemotherapeutic treatments, with a 5-year overall survival rate of about 25%; the development of new targeted treatments therefore represents a key strategy to improve patients' prospects.

The dataset analyzed here includes protein and phosphoproteins levels for 256 newly diagnosed AML patients and is provided as a supplement to [18]. In addition, subjects are classified according to the French-American-British (FAB) system into several different AML subtypes. The dataset contains the levels of $q = 18$ proteins and phosphoproteins involved in apoptosis and cell cycle regulation according to the KEGG database [17].

This data is analyzed by [28] and [6] from a multiple graphical model perspective to estimate group-specific dependence structures based on undirected and directed graphs respectively. Additionally [10] utilize this dataset for Bayesian graphical modeling to examine heterogeneous causal effects.

We focus on subtype M2 and $n = 68$ samples from R package BCDAG. We run the MCMC algorithm with fixed parameters $S = 60000$, $B = 5000$, $a = q$, $U = \frac{1}{n}\mathbf{I}_q$, and $w = 0.5$.

The trace plot of the number of edges in the graphs visited by the MCMC at each iteration $s = 1, \dots, S$ is shown in the left-side panel of Figure 3, and the trace plot demonstrating the average number of edges in the DAGs visited

by the MCMC up to iteration s , for $s = 1, \dots, S$, is shown in the right-side panel.

The apparent absence of trends in the trace plot and the curve stabilization around an average value both suggest a good degree of MCMC mixing and convergence to the target distribution. Also Figure 3 (right panel) shows that the average number of edges in the DAGs is around 22.

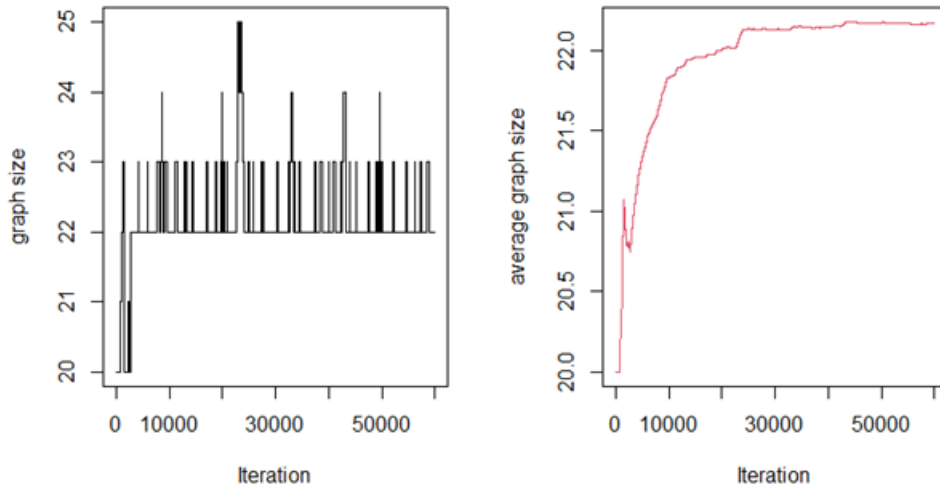


Figure 3: Trace plot of the number of edges (graph size) in the DAGs visited by the MCMC at each iteration (left panel) and trace plot of the average number of edges in the DAGs computed up to iteration s , $s = 1, \dots, 60000$ (right panel) for AML data.

Now we use the MCMC output to estimate the posterior probability of inclusion for each directed edge $u \rightarrow v$, that we report in the heatmap shown in Figure 4.

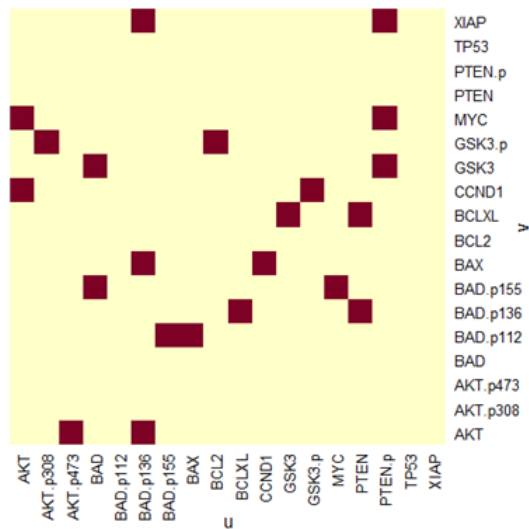


Figure 4: Leukemia data. Heat map with posterior probabilities of edge inclusion, for each directed edge $u \rightarrow v$.

Single DAG estimates that summarize the MCMC output can also be retrieved. For instance consider the maximum a posteriori (MAP) DAG estimate, which corresponds to the DAG with the highest estimated posterior probability. Alternatively, we can create the median probability model (MPM) by including any edges $u \rightarrow v$ with an estimated probability of inclusion greater than 0.5.

Figures 5 and 6 depict the MPM and MAP DAG estimates, respectively.

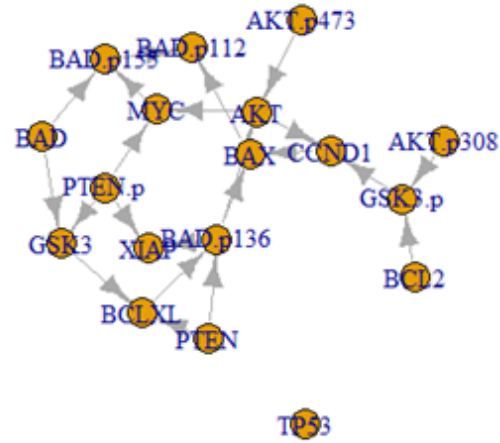


Figure 5: The MPM estimate for AML dataset.

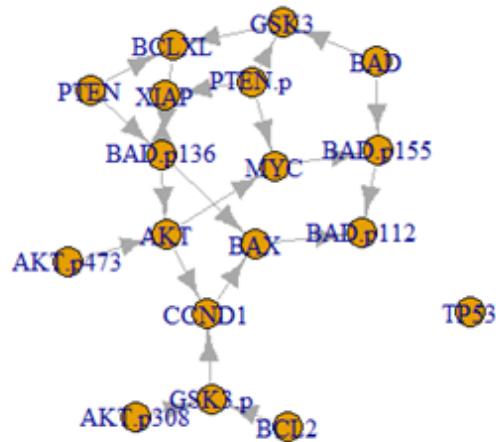


Figure 6: The MAP estimate for AML dataset.

The Maximum A Posteriori (MAP) model estimate is defined as the DAG visited by the MCMC with the highest associated posterior probability. The

posterior probability of each DAG is estimated as the frequency of visits of the DAG in the MCMC chain. The MAP estimate is represented by its $q \times q$ adjacency matrix, with (u, v) element equal to one whenever the MAP contains $u \rightarrow v$, zero otherwise.

The posterior probabilities corresponding to the NIG and NG models are 0.0016 and 0.769, respectively. It is evident that the posterior probability for our NG model is much higher compared to the NIG model.

6. Conclusion

This study presented a technique for learning the relationships between variables by utilizing Bayesian Directed Acyclic Graphs (DAGs) with the non-conjugate normal-gamma (NG) prior. Simulation experiments indicated that the suggested model is conservative in terms of edge inclusion. This means that it tends to construct sparse DAGs when the chance of including edges is low. We classified it as an adaptive Bayesian structure learning approach, where edges are included in the DAG if the inclusion probability adjusts to the true model. Our simulation studies have shown that our model produces a maximum a posteriori DAG (MAP DAG) with a higher posterior probability. Furthermore, our model outperforms the conjugate normal-inverse gamma (NIG) prior in terms of graphical metrics for learning the structure of Gaussian DAGs. In addition, our Bayesian technique exhibits reduced computational time for learning DAGs compared to the NIG prior. Our concept has potential applications in the fields of causal discovery and estimation.

Appendix

In this section, we provide the proof of Theorem 1. To accomplish this, we first give some technical tools, as follows.

Let $\mathbf{x}, \mathbf{b} \in \mathbb{R}^d$ be two vectors, $\mathbf{M} \in \mathbb{R}^{d \times d}$ a symmetric and invertible matrix. Then it can be seen easily that

$$\mathbf{x}^T \mathbf{M} \mathbf{x} - 2\mathbf{b}^T \mathbf{x} = (\mathbf{x} - \mathbf{M}^{-1}\mathbf{b})^T \mathbf{M} (\mathbf{x} - \mathbf{M}^{-1}\mathbf{b}) - \mathbf{b}^T \mathbf{M}^{-1}\mathbf{b}. \quad (A1)$$

Let $K_a(\cdot)$ be the Bessel function of the third kind ([15]). Then for $\text{Re}(\alpha) > 0$, $\text{Re}(\beta) > 0$, (where $\text{Re}(\cdot)$ denotes the real part of a number)

$$\int_0^\infty u^{a-1} \exp\left(-\frac{\alpha}{u} - \beta u\right) du = 2K_a\left(2\sqrt{\alpha\beta}\right) \left(\frac{\alpha}{\beta}\right)^{\frac{a}{2}}. \quad (A2)$$

Proof of Theorem 1. By definition, using (4) and (6), we have

$$\begin{aligned}
m(\mathbf{X}_j | \mathbf{X}_{pa_{\mathcal{D}}(j)}, \mathcal{D}) &= \int_0^\infty \int_{\mathbb{R}^{|pa_{\mathcal{D}}(j)|}} p(\mathbf{D}_{jj}, \mathbf{L}_{\prec j} | \mathcal{D}) f(\mathbf{X}_j | \mathbf{X}_{pa_{\mathcal{D}}(j)}, \mathbf{D}_{jj}, \mathbf{L}_{\prec j}, \mathcal{D}) d\mathbf{L}_{\prec j} d\mathbf{D}_{jj} \\
&= \int_0^\infty \int_{\mathbb{R}^{|pa_{\mathcal{D}}(j)|}} p(\mathbf{L}_{\prec j} | \mathbf{D}_{jj}, \mathcal{D}) p(\mathbf{D}_{jj} | \mathcal{D}) f(\mathbf{X}_j | \mathbf{X}_{pa_{\mathcal{D}}(j)}, \mathbf{D}_{jj}, \mathbf{L}_{\prec j}, \mathcal{D}) d\mathbf{L}_{\prec j} d\mathbf{D}_{jj} \\
&= \int_0^\infty \int_{\mathbb{R}^{|pa_{\mathcal{D}}(j)|}} (2\pi)^{-\frac{n}{2}} |\mathbf{D}_{jj} \mathbf{I}_n|^{-\frac{1}{2}} \\
&\quad \times \exp\left\{-\frac{1}{2} (\mathbf{X}_j + \mathbf{X}_{pa_{\mathcal{D}}(j)} \mathbf{L}_{\prec j})^T (\mathbf{D}_{jj} \mathbf{I}_n)^{-1} (\mathbf{X}_j + \mathbf{X}_{pa_{\mathcal{D}}(j)} \mathbf{L}_{\prec j})\right\} \\
&\quad \times \frac{\left(\frac{1}{2} \mathbf{U}_{jj|pa_{\mathcal{D}}(j)}\right)^{\frac{1}{2} \alpha_j^{\mathcal{D}}}}{\Gamma\left(\frac{1}{2} \alpha_j^{\mathcal{D}}\right)} \times \mathbf{D}_{jj}^{\frac{1}{2} \alpha_j^{\mathcal{D}} - 1} \exp\left\{-\frac{\mathbf{U}_{jj|pa_{\mathcal{D}}(j)}}{2} \mathbf{D}_{jj}\right\} \times (2\pi)^{-\frac{|pa_{\mathcal{D}}(j)|}{2}} \left|\mathbf{D}_{jj} \mathbf{U}_{\prec j}^{-1}\right|^{-\frac{1}{2}} \\
&\quad \times \exp\left\{-\frac{1}{2} (\mathbf{L}_{\prec j} + \mathbf{U}_{\prec j}^{-1} \mathbf{U}_{\prec j})^T (\mathbf{D}_{jj} \mathbf{U}_{\prec j}^{-1})^{-1} (\mathbf{L}_{\prec j} + \mathbf{U}_{\prec j}^{-1} \mathbf{U}_{\prec j})\right\} d\mathbf{L}_{\prec j} d\mathbf{D}_{jj} \\
&= \int_0^\infty \int_{\mathbb{R}^{|pa_{\mathcal{D}}(j)|}} (2\pi)^{-\frac{n+|pa_{\mathcal{D}}(j)|}{2}} \times \mathbf{D}_{jj}^{\frac{1}{2} \alpha_j^{\mathcal{D}} - \frac{|pa_{\mathcal{D}}(j)|}{2} - \frac{n}{2} - 1} \times |\mathbf{U}_{\prec j}|^{\frac{1}{2}} \\
&\quad \times \frac{\left(\frac{1}{2} \mathbf{U}_{jj|pa_{\mathcal{D}}(j)}\right)^{\frac{1}{2} \alpha_j^{\mathcal{D}}}}{\Gamma\left(\frac{1}{2} \alpha_j^{\mathcal{D}}\right)} \times \exp\left\{-\frac{\mathbf{U}_{jj|pa_{\mathcal{D}}(j)}}{2} \mathbf{D}_{jj}\right\} \\
&\quad \times \exp\left\{-\frac{1}{2} (\mathbf{X}_j + \mathbf{X}_{pa_{\mathcal{D}}(j)} \mathbf{L}_{\prec j})^T (\mathbf{D}_{jj} \mathbf{I}_n)^{-1} (\mathbf{X}_j + \mathbf{X}_{pa_{\mathcal{D}}(j)} \mathbf{L}_{\prec j})\right. \\
&\quad \left. - \frac{1}{2} (\mathbf{L}_{\prec j} + \mathbf{U}_{\prec j}^{-1} \mathbf{U}_{\prec j})^T (\mathbf{D}_{jj} \mathbf{U}_{\prec j}^{-1})^{-1} (\mathbf{L}_{\prec j} + \mathbf{U}_{\prec j}^{-1} \mathbf{U}_{\prec j})\right\} d\mathbf{L}_{\prec j} d\mathbf{D}_{jj}
\end{aligned}$$

Let $\mathbf{M} = \tilde{\mathbf{U}}_{\prec j} = \mathbf{U}_{\prec j} + \mathbf{X}_{pa_{\mathcal{D}}(j)}^T \mathbf{I}_n \mathbf{X}_{pa_{\mathcal{D}}(j)}$, and $\mathbf{b} = -\mathbf{X}_{pa_{\mathcal{D}}(j)}^T \mathbf{I}_n \mathbf{X}_j - \mathbf{U}_{\prec j}$, by using (A1) we have

$$\begin{aligned}
&(\mathbf{L}_{\prec j} + \mathbf{U}_{\prec j}^{-1} \mathbf{U}_{\prec j})^T \mathbf{U}_{\prec j} (\mathbf{L}_{\prec j} + \mathbf{U}_{\prec j}^{-1} \mathbf{U}_{\prec j}) + (\mathbf{X}_j + \mathbf{X}_{pa_{\mathcal{D}}(j)} \mathbf{L}_{\prec j})^T \mathbf{I}_n (\mathbf{X}_j + \mathbf{X}_{pa_{\mathcal{D}}(j)} \mathbf{L}_{\prec j}) \\
&= \mathbf{L}_{\prec j}^T (\mathbf{U}_{\prec j} + \mathbf{X}_{pa_{\mathcal{D}}(j)}^T \mathbf{I}_n \mathbf{X}_{pa_{\mathcal{D}}(j)}) \mathbf{L}_{\prec j} + 2 (\mathbf{X}_j^T \mathbf{I}_n \mathbf{X}_{pa_{\mathcal{D}}(j)} + \mathbf{U}_{\prec j}^T) \mathbf{L}_{\prec j} \\
&+ \mathbf{U}_{\prec j}^T \mathbf{U}_{\prec j}^{-1} \mathbf{U}_{\prec j} + \mathbf{X}_j^T \mathbf{I}_n \mathbf{X}_j \\
&= (\mathbf{L}_{\prec j} - \mathbf{M}^{-1} \mathbf{b})^T \mathbf{M} (\mathbf{L}_{\prec j} - \mathbf{M}^{-1} \mathbf{b}) - \mathbf{b}^T \mathbf{M}^{-1} \mathbf{b} + \mathbf{U}_{\prec j}^T \mathbf{U}_{\prec j}^{-1} \mathbf{U}_{\prec j} + \mathbf{X}_j^T \mathbf{I}_n \mathbf{X}_j
\end{aligned}$$

Therefore, we obtain

$$\begin{aligned}
m(\mathbf{X}_j \mid \mathbf{X}_{pa_{\mathcal{D}}(j)}, \mathcal{D}) &= \int_0^\infty \int_{\mathbb{R}^{|pa_{\mathcal{D}}(j)|}} (2\pi)^{-\frac{n+|pa_{\mathcal{D}}(j)|}{2}} \times \mathbf{D}_{jj}^{\frac{1}{2}\alpha_j^{\mathcal{D}} - \frac{|pa_{\mathcal{D}}(j)|}{2} - \frac{n}{2} - 1} \times |\mathbf{U}_{\prec j \succ}|^{\frac{1}{2}} \times \frac{\left(\frac{1}{2}\mathbf{U}_{jj|pa_{\mathcal{D}}(j)}\right)^{\frac{1}{2}\alpha_j^{\mathcal{D}}}}{\Gamma\left(\frac{1}{2}\alpha_j^{\mathcal{D}}\right)} \\
&\times \exp\left\{-\frac{\mathbf{U}_{jj|pa_{\mathcal{D}}(j)}}{2}\mathbf{D}_{jj} - \frac{1}{2\mathbf{D}_{jj}}\left[(\mathbf{L}_{\prec j} - \mathbf{M}^{-1}\mathbf{b})^T \mathbf{M}(\mathbf{L}_{\prec j} - \mathbf{M}^{-1}\mathbf{b})\right. \right. \\
&\left. \left. - \mathbf{b}^T \mathbf{M}^{-1}\mathbf{b} + \mathbf{U}_{\prec j}^T \mathbf{U}_{\prec j}^{-1} \mathbf{U}_{\prec j} + \mathbf{X}_j^T \mathbf{I}_n \mathbf{X}_j\right]\right\} d\mathbf{L}_{\prec j} d\mathbf{D}_{jj}
\end{aligned}$$

Integrating with respect to $\mathbf{L}_{\prec j}$ and \mathbf{D}_{jj} respectively, using (A2) gives the required result.

■

Acknowledgments

Mohammad Arashi's work is based on the research supported in part by the Iran National Science Foundation (INSF) grant No. 4015320.

References

- [1] Andersson, S. A., Madigan, D., & Perlman, M. D. (1997). A characterization of Markov equivalence classes for acyclic digraphs. *The Annals of Statistics*, 25(2), 505-541.
- [2] Bekker, A., van Niekerk, J. and Arashi, M. (2017) Wishart distribution: Advances in theory with Bayesian application, *Journal of Multivariate Analysis*, 155, 272-283.
- [3] Ben-David, E., Li, T., Massam, H., & Rajaratnam, B. (2015). High dimensional Bayesian inference for Gaussian directed acyclic graph models. arXiv:1109.4371.
- [4] Castelletti, F., Consonni, G., Della Vedova, M. L., & Peluso, S. (2018). Learning Markov equivalence classes of directed acyclic graphs: an objective Bayes approach.

- [5] Castelletti, F. (2020). Bayesian model selection of Gaussian directed acyclic graph structures. *International Statistical Review*, 88(3), 752-775.
- [6] Castelletti, F., La Rocca, L., Peluso, S., Stingo, F. C., & Consonni, G. (2020). Bayesian learning of multiple directed networks from observational data. *Statistics in Medicine*, 39(30), 4745-4766.
- [7] Castelletti, F., & Consonni, G. (2021). Bayesian causal inference in probit graphical models. *Bayesian Analysis*, 16(4), 1113-1137.
- [8] Castelletti, F., & Mascaro, A. (2021). Structural learning and estimation of joint causal effects among network-dependent variables. *Statistical Methods & Applications*, 30, 1289-1314.
- [9] Castelletti, F., & Mascaro, A. (2022). Bcdag: An r package for bayesian structure and causal learning of gaussian dags. arXiv:2201.12003.
- [10] Castelletti, F., & Consonni, G. (2023). Bayesian graphical modeling for heterogeneous causal effects. *Statistics in Medicine*, 42(1), 15-32.
- [11] Cooper, G. F., & Herskovits, E. (1992). A Bayesian method for the induction of probabilistic networks from data. *Machine Learning*, 9, 309-347.
- [12] Erdelyi, A., Magnus, W., Oberhettinger, F., & Tricomi, F.G. (1953). *Higher transcendental functions I*. United States of America: McGraw-Hill Inc.
- [13] Friedman, N., & Koller, D. (2003). Being Bayesian about network structure. A Bayesian approach to structure discovery in Bayesian networks. *Machine Learning*, 50, 95-125.
- [14] Geiger, D., & Heckerman, D. (2002). Parameter priors for directed acyclic graphical models and the characterization of several probability distributions. *The Annals of Statistics*, 30(5), 1412-1440.
- [15] Gradshteyn, I.S. and Ryzhik, I.M. (2007). *Table of integrals, series and products*. United States of America: Academic Press.

- [16] Kalisch, M., & Bühlman, P. (2007). Estimating high-dimensional directed acyclic graphs with the PC-algorithm. *Journal of Machine Learning Research*, 8(3).
- [17] Kanehisa, M., Goto, S., Sato, Y., Furumichi, M., & Tanabe, M. (2012). KEGG for integration and interpretation of large-scale molecular data sets. *Nucleic Acids Research*, 40(D1), D109-D114.
- [18] Kornblau, S. M., Tibes, R., Qiu, Y. H., Chen, W., Kantarjian, H. M., Andreeff, M., ... & Mills, G. B. (2009). Functional proteomic profiling of AML predicts response and survival. *Blood, The Journal of the American Society of Hematology*, 113(1), 154-164.
- [19] Lauritzen, S. L. (1996). *Graphical Models*. Oxford University Press.
- [20] Maathuis, M. & Nandy, P. (2016). A review of some recent advances in causal inference. In P. Bühlmann, P. Drineas, M. Kane & M. van der Laan, eds., *Handbook of Big Data*. Chapman and Hall/CRC, 387–408.
- [21] Mohammadi, A., & Wit, E. C. (2015). Bayesian structure learning in sparse Gaussian graphical models.
- [22] Mohammadi, R., & Wit, E. C. (2015). BDgraph: An R package for Bayesian structure learning in graphical models. arXiv:1501.05108.
- [23] Ni, Y., Stingo, F. C., & Baladandayuthapani, V. (2017). Sparse multi-dimensional graphical models: A unified Bayesian framework. *Journal of the American Statistical Association*, 112(518), 779-793.
- [24] Pearl, J. (2000). *Causality: Models, Reasoning, and Inference*. Cambridge University Press, Cambridge.
- [25] Pearl J (2009) *Causality*. Cambridge University Press, Cambridge.
- [26] Peters, J., & Bühlmann, P. (2014). Identifiability of Gaussian structural equation models with equal error variances. *Biometrika*, 101(1), 219-228.
- [27] Peters, J., Janzing, D. & Schölkopf, B. (2017). *Elements of Causal Inference: Foundations and Learning Algorithms*. The MIT Press.

- [28] Peterson, C., Stingo, F. C., & Vannucci, M. (2015). Bayesian inference of multiple Gaussian graphical models. *Journal of the American Statistical Association*, 110(509), 159-174.
- [29] Sachs, K., Perez, O., Pe'er, D., Lauffenburger, D. A., & Nolan, G. P. (2005). Causal protein-signaling networks derived from multiparameter single-cell data. *Science*, 308(5721), 523-529.
- [30] Shimizu, S., Hoyer, P. O., Hyvärinen, A., Kerminen, A., & Jordan, M. (2006). A linear non-Gaussian acyclic model for causal discovery. *Journal of Machine Learning Research*, 7(10), 2003-2030.
- [31] Spirtes, P., Glymour, C. & Scheines, R. (2000). *Causation, Prediction and Search* (2nd edition). Cambridge, MA: The MIT Press.
- [32] Solus, L., Wang, Y., & Uhler, C. (2021). Consistency guarantees for greedy permutation-based causal inference algorithms. *Biometrika*, 108(4), 795-814.
- [33] Tsamardinos, I., Brown, L. E., & Aliferis, C. F. (2006). The max-min hill-climbing Bayesian network structure learning algorithm. *Machine Learning*, 65, 31-78.
- [34] Vogels, L., Mohammadi, R., Schoonhoven, M., & Birbil, Ş. İ. (2023). Bayesian Structure Learning in Undirected Gaussian Graphical Models: Literature Review with Empirical Comparison. arXiv:2307.02603.